Bioorganic Chemistry 57 (2014) 5–12

Contents lists available at ScienceDirect

Bioorganic Chemistry

journal homepage: www.elsevier.com/locate/bioorg

Synthesis of copper/nickel nanoparticles using newly synthesized Schiff-base metals complexes and their cytotoxicity/catalytic activities

Elham S. Aazam [a], Waleed Ahmed El-Said [b,*]

[a] Department of Chemistry, Girls Campus, King Abdulaziz University, P.O. Box 6171, Jeddah 21442, Saudi Arabia
[b] Department of Chemistry, Faculty of Science, Assiut University, Assiut 71516, Egypt

ARTICLE INFO

Article history:
Received 7 April 2014
Available online 30 July 2014

Keywords:
Schiff-base
Copper and nickel nanoparticles
Anticancer activity
Antibacterial efficiency
Nitrobenzene hydrogenation

ABSTRACT

Transition metal complexes compounds with Schiff bases ligand representing an important class of compounds that could be used to develop new metal-based anticancer agents and as precursors of metal NPs. Herein, 2,3-bis-[(3-ethoxy-2-hydroxybenzylidene)amino]but-2-enedinitrile Schiff base ligand and its corresponding copper/nickel complexes were synthesized. Also, we reported a facile and rapid method for synthesis nickel/copper nanoparticles based on thermal reduction of their complexes. Free ligand, its metal complexes and metals nanoparticles have been characterized based on elemental analysis, transmission electron microscopy, powder X-ray diffraction, magnetic measurements and by various spectroscopic (UV–vis, FT-IR, ^{1}H NMR, GC–MS) techniques. Additionally, the in vitro cytotoxic activity of free ligand and its complexes compounds were assessed against two cancer cell lines (HeLa and MCF-7 cells)and one healthy cell line (HEK293 cell). The copper complex was found to be active against these cancer cell lines at very low LD_{50} than the free ligand, while nickel complex did not show any anticancer activity against these cell lines. Also, the antibacterial activity of as-prepared copper nanoparticles were screened against *Escherichia coli*, which demonstrated *minimum inhibitory concentration* and *minimum bactericidal concentration* values lower than those values of the commercial Cu NPs as well as the previous reported values. Moreover, the synthesized nickel nanoparticles demonstrated remarkable catalytic performance toward hydrogenation of nitrobenzene that producing clean aniline with high selectivity (98%). This reactivity could be attributed to the high degree of dispersion of Ni nanoparticles.

1. Introduction

Schiff bases have been used in a multitude of different applications areas such as medical, biological and catalysis applications [1,2]; in addition to its broad spectrum of biological activities such as antiviral, antifungal, antiparasitic, antibacterial, anti-inflammatory, antitumor, anti-HIV, and anticancer [3,4]. Moreover, Schiff base compounds could be operated as important intermediates in enzymatic reactions or inhibitors of the enzymatic actions due to their structural similarity to biological systems [5]. Generally, the transition metals have been known to possess an important role in living organism. Moreover, their complexes with Schiff-base ligands were reported to have high anticancer activity in compare to the free ligands [6]. Particularly, complexes of tetradentate Schiff base ligands (N_2O_2) with transition metals (such as manganese, copper and nickel) found to have antibacterial, antifungal and cytotoxicity activity [7–9]. The transition metal complexes, which could interact with the nucleic acid (by intercalation, groove-binding or electrostatic attraction) have been reported [10,11]. Copper complexes compounds have proved to be one of the most metallic species that have wide anticancer activity due to the selective permeability of cancer cell membranes to copper compounds [12,13]. In our provisos work, we have reported the ability of Cu^{2+} to interact with single strand DNA based on a chelation with the nearby phosphate groups [14]. Therefore, there is increasing interest in the development of new Schiff bases complexes with different transition metal, which could act as anticancer agents based on the cleaving of the cancer cells DNA under physiological conditions [15,16].

Magnetic nanoparticles (MNPs) have recently attracted increasing attention due to their unique properties and applications in different fields [17–19]. In our recent work we have reported the application of the hydrothermal method for synthesis of NiO NPs from nano-sized Ni(II) Schiff-base complex as a precursor [20]. Currently, Ni NPs become one of the most interesting magnetic transition metal-based materials due to its promising potential applications in catalysts [21], capacitor and magnetic materials

* Corresponding author. Fax: +20 882342708.
E-mail address: waleed@sogang.ac.kr (W.A. El-Said).

http://dx.doi.org/10.1016/j.bioorg.2014.07.004
0045-2068/

[22,23]. Ni NPs were prepared by using different methods such as ball milling, electrodeposition, thermal plasma, chemical vapor deposition and chemical reduction in the liquid phase [24,25]. However, it is difficult to obtain pure metallic Ni nanostructures due to their high ability to oxidize [26]. Thermal reduction technique was reported to have many advantages for large-scale synthesis at the industrial level and it offered the advantage of producing essentially pure metal NPs in a solid state without using any other protective agents such as polyvinylpyrrolidone, polyvinyl alcohol, oleic acid or cetyltrimethyl ammonium bromide that could be adsorbed on the surface of NPs; thus, alter their electronic and magnetic properties [27].

Catalytic hydrogenation of aromatic nitro compounds is an important process for the synthesis of amino compounds such as aniline. These compounds are widely used in the production of herbicide, dyes, pigments and pharmaceutical applications. Hydrogenation of nitrobenzene is usually catalyzed by supported expensive noble metals (Pt, Pd, and Ru) or with cheap Raney Ni (100-fold cheaper than Pd and Ru) [28].

This work aims to develop new Schiff base ligand and its tetradentate (N_2O_2) complexes with transition metals (Cu and Ni) to investigate their different applications that including their potentiality as anticancer agents and as precursors for synthesis of metal nanostructures; in addition to study the applications of the results metal nanostructures.

Herein, we have reported the synthesis of new Schiff base ligand from the condensation reaction of 3-ethoxy-2-hydroxybenzaldehyde with 2,3-Diaminobut-2-ene-dinitrile as tetradentate (N_2O_2) ligand. The Cu(II) and Ni(II) complexes of this ligand were also prepared. The in vitro cytotoxicity of the free Schiff bases ligand and its complexes against two human carcinoma cell lines (HeLa and MCF-7) has been investigated. In addition, we used these Schiff-base complexes for rapid preparation of pure face-centered cubic (fcc) Ni NPs and Cu NPs based on thermal reduction method. The size, surface area and structure of the resultant NPs were characterized by transmission electron microscopy (TEM), powder X-ray diffraction (XRD) and N_2-adsorption. In addition, the magnetic properties of the prepared Ni NPs were measured by using vibrating sample magnetometer (VSM), which exhibited ferromagnetic properties with a saturation magnetization of 48.1 emu/g, a remnant magnetization of 4.1 emu/g and a coercivity of 104.2 Oe at room temperature. Moreover, the antibacterial activity of as-prepared Cu NPs against *E. Coli* of the as-prepared Cu NPs was investigated. Finally, the catalytic performance of the prepared Ni NPs toward hydrogenation of nitrobenzene to aniline was evaluated based on GC–MS, which demonstrated high activity and selectivity of the synthesized Ni NPs.

2. Experimental

2.1. Materials

2,3-Diaminobut-2-ene-dinitrile and 3-ethoxy-2-hydroxybenzaldehyde were purchased from Aldrich; while, nickel acetate tetrahydrate and copper acetate dihydrate were obtained from BDH. The other chemicals used in this study were obtained commercially as reagent grade. All solutions were prepared with distilled Millipore (Milli-Q) water.

2.2. Physical measurements

Elemental analysis was determined in the Micro Analytical Unit using Perkin Elmer 2400 (London, Metropolitan University, UK). Infrared (IR) spectra of solids were recorded on a Perkin Elmer 100 FT-IR spectrophotometer. UV–vis spectra were recorded on a Varian 2300 spectrophotometer. ^{1}H NMR spectra were recorded on a Varian 500 MHz spectrometer. The ^{1}H NMR chemical shifts (δ, ppm) were given relative to the residual solvent peaks. TEM images were recorded using a JEOL-JEM-1230 microscope. The synthesized Ni or Cu NPs were suspending in ethanol, followed by ultrasonication for 30 min. Then, a drop of the suspension was added to a carbon coated copper grid allowing the solvent to be evaporated before its introduction into the TEM. X-ray diffraction (XRD) analysis was carried out at room temperature using a Bruker axis D8 using Cu Kα radiation (λ = 1.540 Å) over a 2θ collection range of 10–80°. The surface area was measured by the BET (Brunauer–Emmett–Teller) method based on N_2-adsorption using Nova 2000 series Chromatech apparatus at 77 K. Prior to the measurements all samples were treated under vacuum at 200 °C for 2 h. Vibration sample magnetometer measurements of the prepared Ni were performed using a Lakeshore 7400 VSM and EM4-HVA electromagnet (EM4-HVA, USA) at room temperature.

2.3. Synthesis of 2,3-bis-[(3-ethoxy-2-hydroxybenzylidene)amino]but-2-enedinitrile (H_2L)

2,3-Diaminobut-2-ene-dinitrile (1.30 g, 12.04 mmol) in 30 mL of methanol was added to a stirred solution of 3-ethoxy-2-hydroxybenzaldehyde (4 g, 24.07 mmol) in 30 mL of methanol. The mixture was refluxed and turned golden-brown after half an hour and a golden-brown precipitate was formed after one hour. The product was collected by filtration as a golden-brown solid. The purity of the product was estimated by TLC {EtOAc-PET (2: 8 V/V)} and ^{1}H NMR spectroscopy. Yield: 59.55%, (2.9 g, 7.17 mmol) and m.p. (170 °C). ^{1}H NMR (DMSO-d6, 500 MHz): δ (ppm) 1.50 (CH_3, 6H, t, J = 6.998), 9.97 (N=CH, 2H), 7.11 (Ar—H, 2H, dd, J = 8.527, J = 8.072), 7.27 (Ar—H, 2H, dd, J = 8.072, J = 1.413), 7.03 (Ar—H, 2H, dd, J = 8.527, J = 1.413), 4.04 (CH_2, 4H, q, J = 6.998) and 11.22 (s, 2H, OH). Anal. Calcd for $C_{22}H_{20}N_4O_4$ [H_2L]: C, 65.34; H, 4.98; N, 13.85. Found (%): C, 65.75; H, 4.30; N, 13.97. Characteristic IR absorptions 3329, 2199, 1601, 1458, 1378, 1251, 1068, 1009, 890, 716 cm^{-1}. UV–vis [DMSO, λ_{max} (nm)]: 230, 275, 420.

2.4. Preparation of 2,3-bis-[(3-ethoxy-2-hydroxybenzylidene)amino]but-2-enedinitrile nickel complex (NiL)

Nickel acetate tetrahydrate (0.198 g, 0.24 mmol) in 20 mL of methanol was added to a stirred solution of H_2L (0.3 g, 0.24 mmol) in 20 mL of methanol. The mixture was refluxed overnight then cooled to room temperature, upon which a dark green precipitate was formed. The product was collected by filtration and washed with 2 mL of methanol, and then air dried. Yield (63.6%, 0.07 g, 0.14 mmol), m.p. decom >360 °C. Anal. Calcd for $C_{22}H_{18}N_4O_4Ni$ [NiL]: C, 57.31; H, 3.93; N, 12.73. Found (%): C, 57.01; H, 3.19; N, 12.18. Characteristic IR absorptions 2222, 1572, 1533, 1446, 1190, 1117, 910, 730 cm^{-1}. UV–vis [DMSO, λ_{max} (nm)]: 430, 458 and 510 nm.

2.5. Preparation of 2,3-bis-[(3-ethoxy-2-hydroxybenzylidene)amino]but-2-enedinitrile copper complex (CuL)

Copper acetate dihydrate (0.153 g, 0.24 mmol) in 20 mL of methanol was added to a stirred solution (0.3 g, 0.24 mmol) of H_2L in 20 mL of methanol. The mixture was refluxed overnight then cooled to room temperature, upon which a green precipitate formed. The product was collected by filtration and washed with 2 mL of methanol, and then air dried. Yield (63.6%, 0.07 g, 0.14 mmol), m.p. decom >360 °C. Anal. Calcd for $C_{22}H_{18}N_4O_4Cu$ [CuL]: C, 56.7; H, 3.86; N, 12.03. Found (%): C, 56.64; H, 3.9; N, 12.1. Characteristic IR absorptions 2222, 1572, 1533, 1446, 1190, 1117, 910, 730 cm^{-1}. UV–vis [DMSO, λ_{max} (nm)]: 400, 478 and 556 nm.

2.6. Preparation of face-centered cubic nickel nanoparticles and copper nanoparticles

The synthesis of pure fcc Ni NPs or Cu NPs were carried out using thermal reduction method [29,30]. Cu(II) complex or Ni(II) complex (1 mmol) was added to 20 ml of triton X-100, which acted as a surfactant agent to create a homogenous solution; followed by the addition of 0.1 mmol of triphenylphosphine (a reducing agent). Then the mixture was stirred under refluxe at 140 °C for one hr. The supernatant was removed and Ni NPs sediments were washed with absolute ethanol and deionized water. Finally, the obtained precipitate was dried in air at 100 °C for 6 h (yield 95%).

2.7. In vitro antibacterial efficiency

E. coli JM109 was used as indicator of model microorganism for the antibacterial studies. The bacteria (6.0 log CFU/mL) were inoculated in Luria Bertani (LB) agar plates supplemented with the prepared Cu NPs and commercial Cu NPs at concentration of 4 and 16 μg/mL, respectively. Plates without Cu NPs and commercial Cu NPs were used as controls. These plates were cultured over 24 h at 35 °C till the numbers of colonies can be observed and counted. All experiments conducted in this study were repeated for 3 times.

2.8. Determination of the minimum inhibitory concentration (MIC) and minimum bactericidal concentration (MBC) of Cu-NPs

E. coli cells were incubated for 20 h in growth medium that containing different concentrations of prepared Cu NPs or commercial Cu NPs and then the viability of the cells before and after incubation was determined by plating. To determine the minimum inhibitory concentration (MIC) and minimum bactericidal concentration (MBC) of Cu-NPs, number of viable cells was detected according to the following protocol. *E. coli* cells were diluted 100 times in fresh LB medium containing different concentrations of prepared Cu NPs and commercial Cu NPs (from 1 μg/mL to 17 μg/mL) and the cultures were allowed to incubate at 37 °C in a gyratory shaker at 125 rpm for 20 h. An amount of 0.1 ml of culture from properly diluted samples was spread over LB agar plates with a glass-spreader and the plates were kept upside down in an incubator at 37 °C until the colonies appeared. The number of colonies multiplied by the dilution factor determined the viable cell counts.

2.9. Cell culture

Human cervical cancer (HeLa), human breast adenocarcinoma (MCF-7) cancer cell lines and human embryonic kidney-293 (HEK-293) healthy cell line were obtained from the Institute of Vaccine and Serum (Cairo, Egypt). HeLa and HEK-293 cells were cultured in Dulbecco's Modified Eagle Medium (DMEM) supplemented with 10% heat inactivated fetal bovine serum (FBS; Gibco, Carlsbad, CA, USA), and a 1% concentration of antibiotics (Gibco). While, MCF-7 cell line was cultured in PRMI (Invitrogen, Carlsbad, USA) with 10% heat-inactivated fetal bovine serum and 2% antibiotics (streptomycin + penicillin). All cell lines were maintained under standard cell culture conditions at 37 °C in an atmosphere of 5% CO_2. The medium was changed every two days.

2.10. Cytotoxicity assay

Cytotoxicity studies of the free Schiff base ligand and its Ni(II) & Cu(II) complexes were carried out on HeLa, HEK-293 and MCF-7 based on the colorimetric MTT assay method. The MTT assay was conducted essentially according to the manufacturer's protocol. HeLa HEK-293and MCF-7 cells at concentration of 2×10^4 -cell/ml were plated and grown in 96-well plates in presence of DMEM medium containing 10% fetal bovine serum (FBS) and incubated at 37 °C, under conditions of 5% CO_2, and 95% air for 24 h prior to the addition of compounds. The compounds were dissolved in dimethyl sulfoxide (DMSO) and diluted in the respective medium containing 1% FBS. Then, cells were treated with different concentrations of free Schiff-base ligand and Schiff-base metal complexes for next 24 h. MTT (0.5 mg/ml) was added to each well and incubated for 4 h. The insoluble formazan was dissolved in 100 μL of DMSO at room temperature for 20 min. Cell viability was assessed by measuring the absorbance at 540 nm using a microplate reader. The results were analyzed by means of cell viability cures and expressed with IC_{50} values as shown in Fig. 7.

2.11. Hydrogenation of nitrobenzene

The hydrogenation of nitrobenzene was carried out in ethanol at 30.0 °C under hydrogen at an atmospheric pressure. The desired amount of the dried catalysts was then dispersed again into a calculated amount of ethanol to form a 0.1 mM ethanol dispersion of metal nanoclusters as catalysts. The catalyst dispersion (20 mL, total metal 2×10^{-6} mol) was injected into a 50 mL flask, where air was thoroughly exchanged in advance by hydrogen at one atmospheric pressure. In this step, the solution containing the catalyst was stirred at 30.0 °C to activate the catalyst. After the initial hydrogenation uptake ceased, 1.0 mL of ethanol solution containing 0.3 mmol of nitrobenzene was added to the flask keeping the total pressure at atmospheric pressure. The hydrogenation products were analyzed with GC–MS (Shimadzu GCMS-QP 5050A).

3. Results and discussion

3.1. Spectroscopic properties of the ligand (H_2L) and its Nickel and Copper complexes

2,3-Bis-[(3-ethoxy-2-hydroxybenzylidene)amino]but-2-enedinitrile (H_2L) ligand was obtained readily by simple mixing of 3-ethoxy-2-hydroxybenzaldehyde and 2,3-Diaminobut-2-ene-dinitrile in alcohol in a 1/1 ratio. Then Cu(II)/Ni(II) complexes were prepared by overnight refluxing of H_2L ligand with the equal molar ration of copper acetate or nickel acetate, respectively in methanol (Scheme 1). ^1H NMR and elemental analysis confirmed the composition of the resulting diimine ligand. Fig. 1 shows the IR spectral data of the Ni and Cu complexes compared to those of the free ligand, which demonstrated that the free ligand showed a broad band characteristic for the OH group at 3329 cm^{-1}. Disappearance of this band in the IR spectra of the complexes is indicative of the fact that the tetradentate N_2O_2 ligand is coordinated as dianions. In addition, loss of a positive hydrogen ion (H^+) from an OH group in the free ligand formed a corresponding negative phenolate ion during complex formation. The (C=N) band appearing at 1601 cm^{-1} in the ligand was shifted to lower frequencies in the corresponding complexes. This indicated that H_2L is coordinated to the metal ion through the N_2O_2 groups. Moreover, IR spectroscopy provided additional evidence for the diimine nature of the compounds with a single band for the CN stretching mode at 2199 and 2222 cm^{-1} for H_2L and ML respectively. This is an indication of the formation of symmetric compounds in contrast to the band split into two components at 2232 and 2206 cm^{-1} for the related unsymmetrical monoimine ligand that was reported previously [31].

UV–vis spectra of the ligand and its Cu/Ni complexes were recorded in DMSO within the range from 200 to 800 nm (Fig. 2). The Schiff-base ligand demonstrated three absorption bands at 230, 275 and 420 nm, which may be attributed to the σ–σ^*, π–π^*

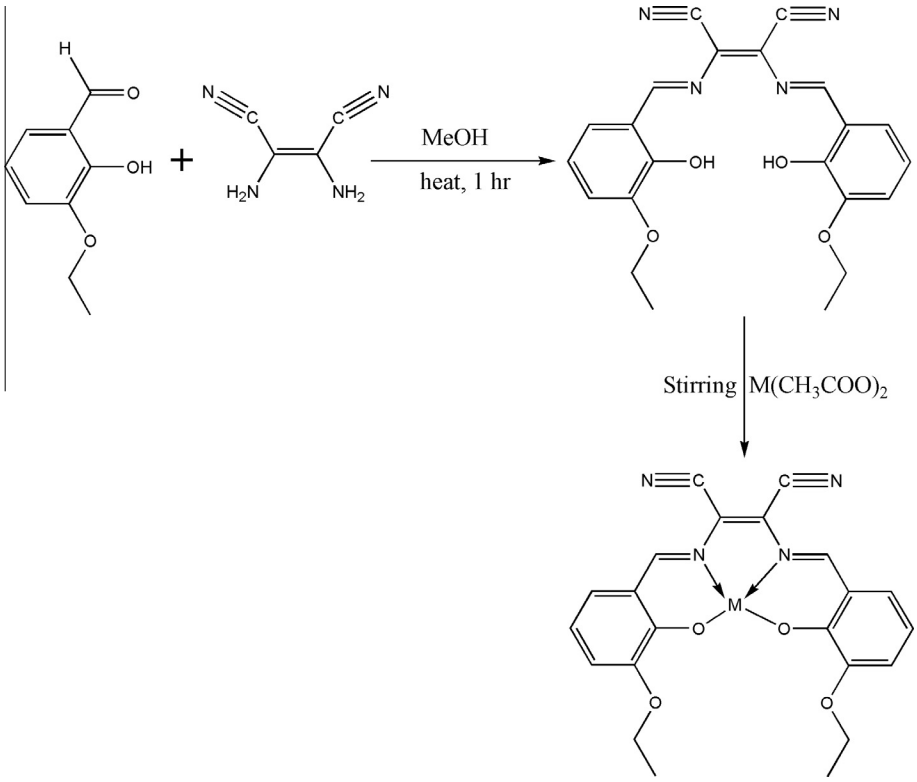

Scheme 1. Synthesis of 2,3-bis-[(3-ethoxy-2-hydroxybenzylidene)amino]but-2-enedinitrile metal complex (ML).

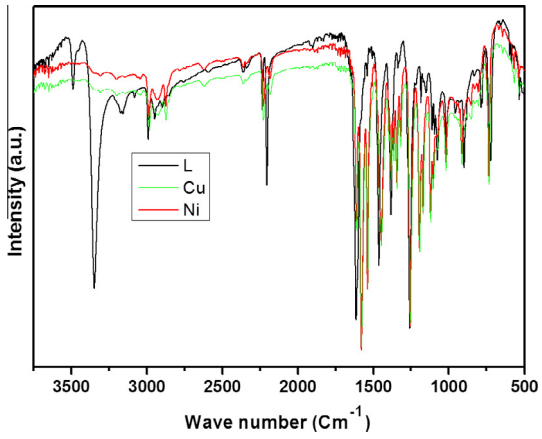

Fig. 1. FT-IR spectra of free N_2O_2 ligand, CuL complex and NiL complex.

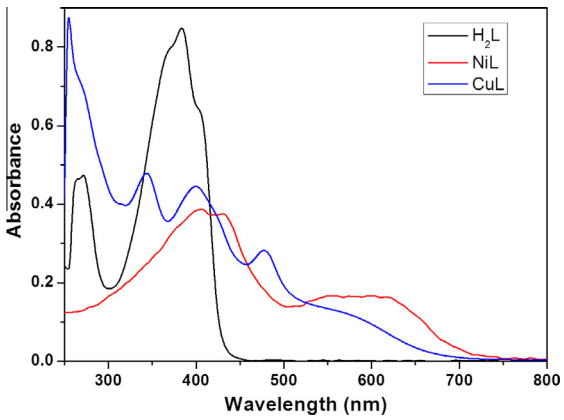

Fig. 2. UV–vis absorption spectra of (black) N_2O_2 free ligand, (blue) CuL complex and (red) NiL complex.

and n–π^* transitions, respectively. In addition, its Ni complex shown three absorption bands at longer wavelength that are corresponding to the transitions $^1A_{1g} \rightarrow {}^1A_{2g}$ (430 nm), $^1A_{1g} \rightarrow {}^1B_{1g}$ (458 nm), and $^1A_{1g} \rightarrow {}^1E_g$ (510 nm).

While, the Cu complex shows three absorption bands at 400 nm, 478 nm and 556 nm corresponding to the transitions $dx^2–y^2 \rightarrow dz^2$, $dx^2–y^2 \rightarrow dxy$, and $dx^2–y^2 \rightarrow dxz$; dyz ($^2A_{1g} \leftarrow {}^2B_{1g}$, $^2B_{2g} \leftarrow {}^2B_{1g}$ and $^2E_g \leftarrow {}^2B_{1g}$), these results indicates the singlet ground state term characteristic of square-planar complexes [32,33].

3.2. Size and morphology of nickel and copper nanoparticles

The size and morphology of the as-prepared Ni NPs and Cu NPs were characterized using TEM as shown in Fig. 3a & b, which demonstrated the formation of irregular Cu and Ni NPs with average size of 25 nm and 28 nm, respectively. The presences of darker particles indicated the ferromagnetic properties of the synthesized Ni NPs. These properties could enhance the diffraction contrast due to their orientation with respect to the electron beam. Moreover, Fig. 3c & d show the isothermals adsorption of nitrogen gas with the prepared Ni NPs and Cu NPs, which demonstrated different behavior. The surface area of the prepared Ni NPs, commercial Raney Ni and Cu NPs samples were determined to be 42, 35 and 33 m^2/g, respectively (Table 1). In addition, the volume of pores for the prepared Ni NPs was significantly greater than that of commercial Raney Ni; while, the value of pore diameter in the prepared Ni NPs is smaller than that found in the commercial Raney Ni (Table 1).

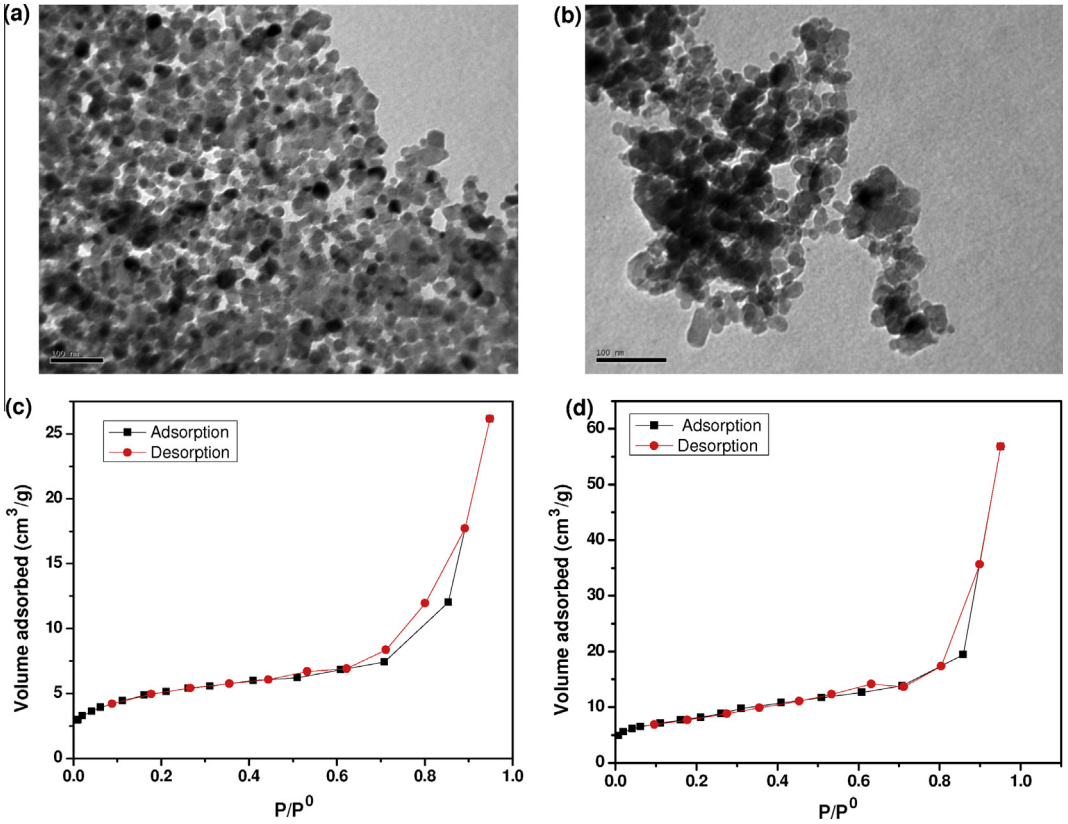

Fig. 3. TEM micrograph of obtained (a) Ni NPs, (b) Cu NPs. N_2 adsorption/desorption isotherms of (c) Ni NPs and (d) Cu NPs.

Table 1
Surface area and porosity of Cu NPs, commercial Ni and Ni NPs, where: S_{BET} is BET-Surface area, V_p is the total pore volume and R is the mean pore radius.

Sample	S_{BET} (m^2/g)	V_p (cm^3/g)	R (Å)
Cu	33	0.140	11.00
Ni	42	0.190	7.00
Commercial Raney Ni	35	0.072	53

3.3. X-ray powder diffraction (XRD) and Raman spectroscopy

Fig. 4a show the corresponding XRD patterns of the resultant Ni and Cu NPs, which demonstrated the presence of three sharp characteristic peaks for Ni ($2\theta = 44.5°$, 51.8°, and 76.4°), corresponding to Miller indices (111), (200) and (222). Also, XRD pattern of Cu showed three peaks at 2θ values of 43.3°, 50.4° and 74.1° corresponding to (111), (200) and (220), respectively. These results indicated the synthesis of stable pure crystalline metallic fcc Ni and Cu NPs [34–36]. Also, appearance of very sharp peaks with high intensity indicated the high nanocrystalline nature of the resulted Cu and Ni NPs. In addition, no impurity peaks or metal oxide peaks could be observed in the XRD patterns. In order to validate our results we have used Raman spectroscopy instrument to analysis the chemical composition of the prepared NPs (Fig. 4b), which did not show any characteristic peaks for the presence of any organic material on the surface of the prepared NPs.

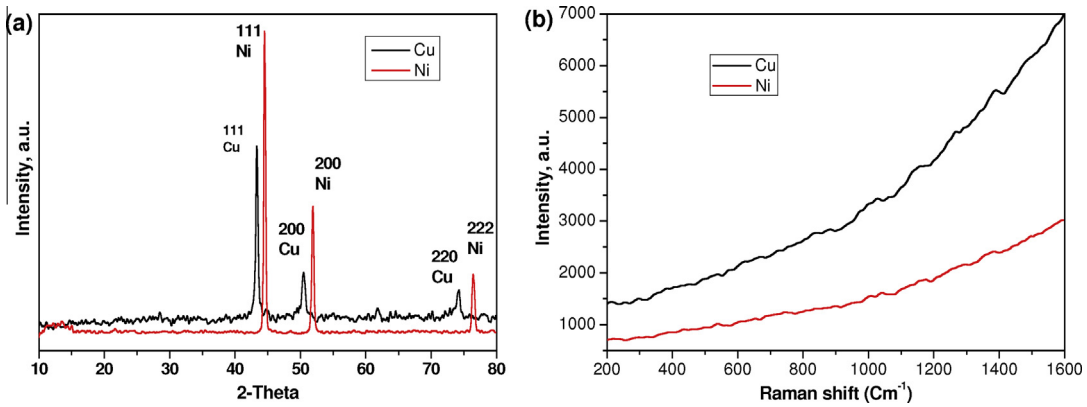

Fig. 4. (a) XRD pattern of obtained fcc Ni and Cu NPs, and (b) Raman spectra of prepared Ni and Cu NPs.

3.4. Magnetic behavior of Ni nanoparticles

Ni has been considered to be one of the most important magnetic materials. Accordingly the magnetic properties of the resultant Ni NPs were investigated using a VSM at room temperature. Fig. 5 demonstrated the magnetic behavior of the synthesized Ni NPs at room temperature that displayed a characteristic hysteresis loop of ferromagnetic materials with a saturation magnetization (*Ms*) of 48.1 emu/g, coercivity (*Hc*) of 104.2 Oe and remnant magnetization (*Mr*) of 4.1 emu/g. Compared to the values of bulk Ni (*Ms* about 55 emu/g, *Hc* about 100 Oe, and *Mr* 2.7 emu/g) [37], the value of *Hc* was enhanced; while, *Ms* was decreased. These findings indicated that the as-prepared Ni NPs are ferromagnetic at room temperature [38]. The reason for these changes may be attributed to the decrease of particle size and the accompanied increase in surface area. Therefore, the above results indicated that the synthesized Ni NPs exhibit typical ferromagnetic characteristics of fcc Ni NPs [25].

3.5. Catalytic hydrogenation of nitrobenzene

Fig. 6 shows the performances of the synthesized Ni NPs and commercial Raney Ni as catalysts in the hydrogenation of nitrobenzene without any catalyst pre-reduction. Linear conversion of nitrobenzene with time since the beginning of the reaction clearly indicated that the Ni NPs were well stable. The catalytic activity of the synthesized Ni NPs demonstrated high selectivity for aniline (98%). Moreover, Fig. 6 demonstrated that the catalytic efficiency of the prepared Ni NPs is slightly higher in comparison to the commercial Raney Ni that could be related to the large surface area, large pore volume and small pore radius of the prepared Ni NPs. In addition, previous studies reported that many intermediates, (e.g. nitrosobenzene, N-phenylhydroxylamine, azoxybenzene, azobenzene, and hydrazobenzene) could be formed during hydrogenation of nitrobenzene [39–41]. However, our results demonstrated that the hydrogenation of nitrobenzene in the presence of the prepared Ni NPs under the reported conditions is selective hydrogenation for aniline. Thus, there is no other intermediates had been detected during the reduction of nitrobenzene. In addition, the magnetic behavior of the prepared Ni nanoparticles provides a simply removing method of the catalyst from the reaction medium by applied external magnetic field.

3.6. Antibacterial efficiency

The efficiency of Cu NPs on bacterial growth was studied by incorporating various concentrations of Cu NPs in LB agar plates

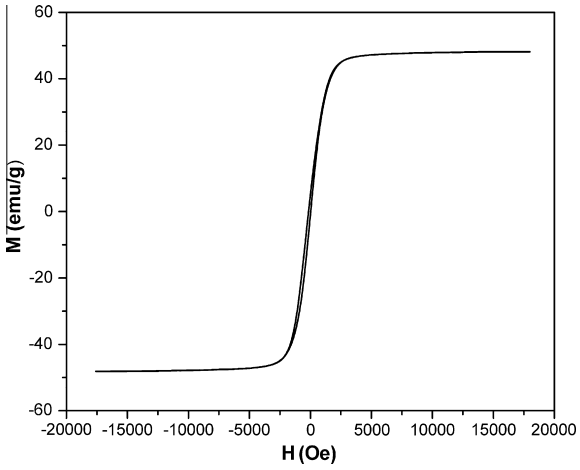

Fig. 5. Hysteresis loop for the obtained fcc Ni NPs at room temperature.

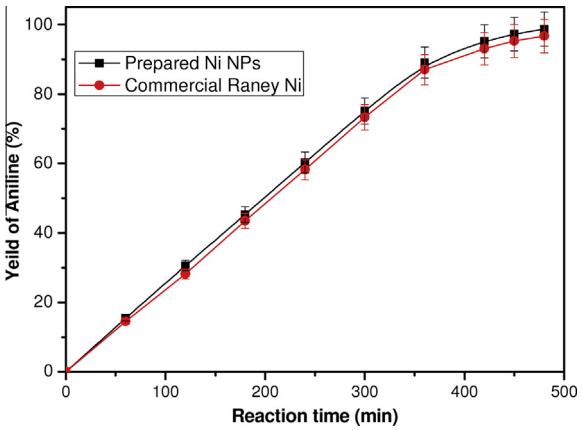

Fig. 6. Performance of Ni NPs as a catalyst in the hydrogenation of nitrobenzene without pre-reduction.

that were inoculated with 6.0 log CFU/mL *E. coli* strain. Furthermore, the same concentrations of commercial Cu NPs were used to compare the antibacterial activity of the prepared Cu NPs. The results show that bacterial growth was significantly reduced by treatment with the synthesized Cu NPs. In addition, the growth of *E. coli* was completely inhibited at concentration of 16 μg/mL of the as-prepared Cu NPs. While, the treatment of *E. coli* with commercial Cu NPs at high concentration (16 μg/mL) could reduce the bacterial grow, but there was still significant growth of *E. coli.* Quantitative difference is clearly showed in the survival count of *E. coli* (Table 2). At high concentration of the commercial Cu NPs, the survival count of *E. coli* was 25 times larger than that of prepared Cu NPs (2.5 log CFU/mL vs 0.1 log CFU/mL). The high antibacterial efficacy of the synthesized Cu NPs over commercial Cu NPs is believed to be the benefit of greatly increased surface area.

Table 3 shows the *E. coli* viability after incubation with different concentrations of prepared Cu-NPs and commercial Cu NPs for 20 h, which demonstrated that the number of viable cells was increased at low concentrations; while, the cells number was decreased after incubation with high concentrations of Cu-NP. Furthermore, these results shows that the MIC of prepared Cu NPs and commercial Cu NPs to *E. coli* was 3.0 and 5.0 μg/mL, respectively. In addition, the MBC values for prepared Cu NPs and commercial Cu NPs to *E. coli* was 10 and 13 μg/mL, respectively. Thus, both the MIC and MBC values of the prepared Cu NPs were lower than those values of the commercial Cu NPs as well as the previous reported values [42,43]. Furthermore, control experiment was also performed without adding Cu NPs to investigate whether the ingredients of the prepared Cu NPs had any antibacterial potency.

3.7. In vitro cytotoxic activities of the free ligand and its metal complexes compounds

Recent studies reported the potential applications of Cu Schiff base complexes for DNA-binding and DNA cleavage [15,16]. Therefore, we have investigate the cytotoxicity activities of free ligand and its metal complexes against two human cancer cell lines namely (HeLa and MCF-7) and one healthy cell line (HEK-293 cells) by using MTT assay in which the cell viability was measured based on the mitochondrial dehydrogenase activity. Free ligand and its metal complexes were dissolved in DMSO and blank samples containing the same volume of DMSO were taken as controls to identify the activity of solvent in this cytotoxicity experiment. The results were analyzed by means of cell viability cures and expressed with IC_{50} values as shown in Fig. 7. The results of the in vitro cytotoxicity activity studies indicate that Cu complex has

Table 2
The antibacterial activity of the compounds against *Escherichia coli*.

Concentration Material	Survival count of *E. coli*			
Prepared Cu nanoparticle (4 μg/mL)	First run 1.9	Second run 2.0	Third run 2.1	Average 2.1
Commercial Cu nanoparticle (4 μg/mL)	First run 3.9	Second run 4	Third run 4.1	Average 4
Prepared Cu nanoparticle (16 μg/mL)	First run 0.11	Second run 0.10	Third run 0.11	Average 0.10
Commercial Cu nanoparticle (16 μg/mL)	First run 2.42	Second run 2.53	Third run 2.57	Average 2.53

Table 3
Number of viable cells after 20 h of incubation with increasing concentration of Cu-NPs. Initial No. of antibiotic-resistant *E. coli* cells (before incubation) was 3.1×10^7.

Concentration of materials (μg/mL)	No. of *E. coli* cells after 20 h incubation with prepared Cu NPs	No. of *E. coli* cells after 20 h incubation with commerical Cu NPs
0	41.4×10^8	42.3×10^8
1	35.2×10^8	39.2×10^8
2	6.1×10^8	26.4×10^8
3	3.1×10^7	3.1×10^8
5	2.5×10^6	2.9×10^7
7	3×10^5	4.2×10^6
10	4.1×10^4	5.4×10^5
13	3.2×10^3	4.2×10^4
15	1.5×10^3	3.8×10^3
17	1.1×10^3	1.5×10^3

the higher cytotoxicity activity than free ligand; while Ni complex did not show any significant activity on the tested cancer cell lines. The IC_{50} values for Cu complex were 14.04 and 19.25 mM for HeLa and MCF-7 cell, respectively, which indicated that the Cu complex exhibits significant activity against HeLa and MCF-7 cell lines. Also, HeLa cells were more sensitive to Cu complex than MCF-7 cells.

In order to validate the anticancer activity of the synthesized Cu-complex, the effects of different synthesized compounds

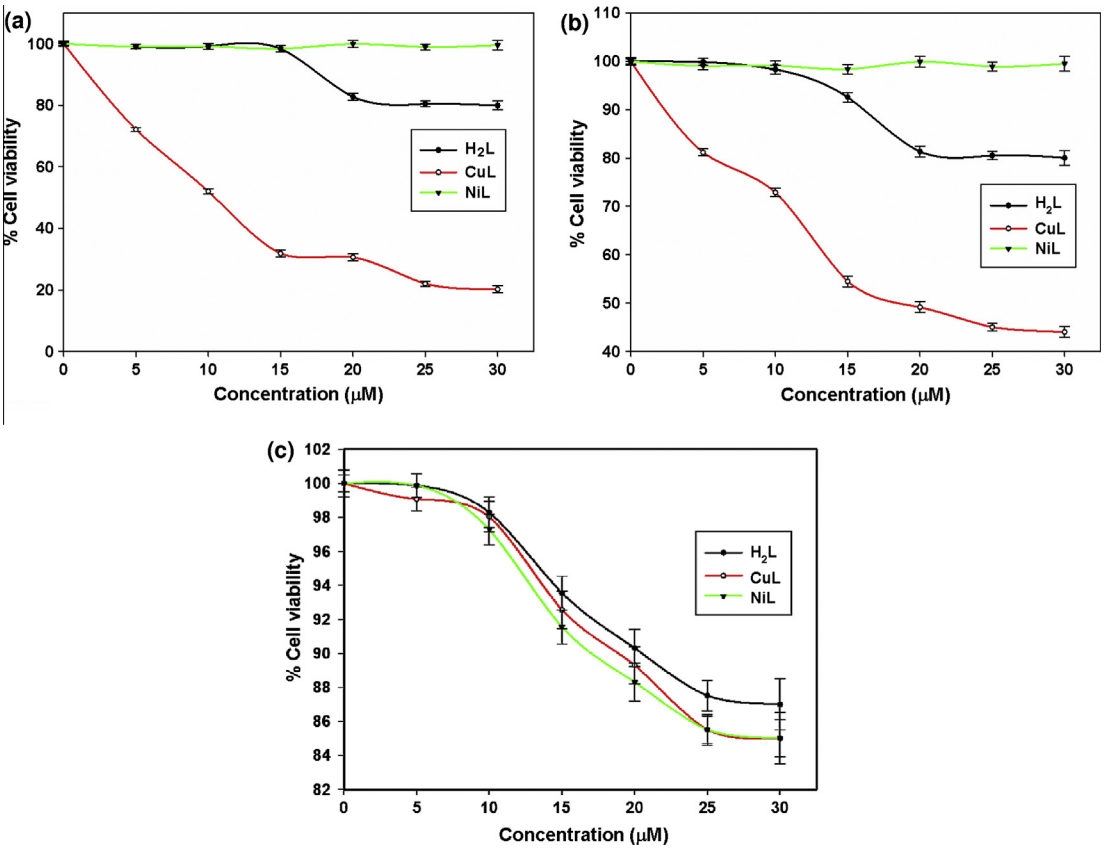

Fig. 7. Cytotoxic effects of free ligand and its Cu & Ni complexes against (a) HeLa cells and (b) MCF-7 cells.

against healthy cell line (HEK-293 cells) was also investigated, which demonstrated that the all prepared samples did not have any significant effect on HEK-293 cell line (Fig. 7c).

4. Conclusions

In this work we have reported the synthesis of a new Schiff-base N_2O_2 ligand and its Ni/Cu complexes. The Cu complex has shown higher anticancer activity rather than the free ligand; while, the Ni complex did not show any significant anticancer activity against HeLa or MCF-7 cancer cells.

Moreover, these metal complexes were used for synthesis of pure fcc Ni and Cu NPs based on thermal reduction of these Schiff-base metal complexes. In addition, the prepared Ni NPs have been demonstrated a remarkable catalytic performance toward hydrogenation of nitrobenzene without a catalyst pre-reduction, producing clean aniline under mild conditions with high selectivity for aniline (98%). Therefore, the prepared Ni NPs could be used as a catalyst in the bulk industrial production of pure amines with the advantage of avoid the accumulation of the hazardous intermediate such as hydroxyl amines that are toxic and its accumulation could be lead to exothermic decomposition and/or formation of condensation products. Furthermore, the as-prepared Cu NPs have shown higher antibacterial activity against *E. coli* in compare to the same concentration of commercial Cu NPs.

Acknowledgments

This paper was funded by the Deanship of Scientific Research (DSR). King Abdulaziz University, Jeddah, under grant No. (173/247/1432). The authors, therefore, acknowledge with thanks DSR technical and financial support.

References

[1] M.I. Mohamed, M.A. Hapipah, A.A. Mahmood, T.R. Ward, Polyhedron 28 (2009) 3993–3998.
[2] Z.-C. Liu, B.-D. Wang, Z.-Y. Yang, Y. Li, D.-D. Qin, T.-R. Li, Eur. J. Med. Chem. 44 (2009) 4477–4484.
[3] E. Toyota, K.K.S. Ng, H. Sekisaki, K. Itoh, K. Tanisawa, M.N.G. James, J. Mol. Biol. 305 (2001) 471–479.
[4] M.D. Shelley, L. Hartley, P.W. Paul, R.G. Fish, Anticancer Drug 11 (2000) 209–216.
[5] B. Chattopadhyay, S. Basu, P. Chakraborty, S.K. Choudhuri, A.K. Mukherjee, M. Mukherjee, J. Mol. Struct. 932 (2009) 90–96.
[6] A. Robertazzi, A. Magistrato, P. de Hoog, P. Carloni, J. Reedijk, Inorg. Chem. 46 (2007) 5873–5881.
[7] B.C. Bales, M. Pitie, B. Meunier, M.M. Greenberg, J. Am. Chem. Soc. 124 (2002) 9062–9063.
[8] M. Nath, P.K. Saini, Dalton Trans. 40 (2011) 7077–7121.
[9] K. Serbest, A. Özen, Y. Ünver, M. Er, I. Değirmencioğlu, K. Sancak, J. Mol. Struct. 922 (2009) 1–10.
[10] V. Barve, F. Ahmed, S. Adsule, S. Banerjee, S. Kulkarni, P. Katiyar, C.E. Anson, A.K. Powell, S. Padhye, F.H. Sarkar, J. Med. Chem. 49 (2006) 3800–3808.
[11] V.C. da Silveira, J.S. Luz, C.C. Oliveira, I. Graziani, M.R. Ciriolo, da Costa, A.M. Ferreira, J. Inorg. Biochem. 102 (2008) 1090–1103.
[12] C. Metcalfe, J.A. Thomas, Chem. Soc. Rev. 32 (2003) 215–224.
[13] K. Jiao, Q.X. Wang, W. Sun, F.F. Jian, J. Inorg. Biochem. 99 (2005) 1369–1375.
[14] T. Lee, W.A. El-Said, J.-H. Min, J.-W. Choi, Biosens. Bioelectron. 26 (2011) 2304–2310.
[15] V. Rajendiran, R. Karthik, M. Palaniandavar, H.S. Evans, V.S. Periasamy, M.A. Akbarsha, B.S. Srinag, H. Krishnamurthy, Inorg. Chem. 46 (2007) 8208–8221.
[16] A. Barve, A. Kumbhar, M. Bhat, B. Joshi, R. Butcher, U. Sonawane, R. Joshi, Inorg. Chem. 48 (2009) 9120–9132.
[17] S. Sun, H. Zeng, J. Am. Chem. Soc. 124 (2002) 8204.
[18] M. Aslam, S. Li, V.P. Dravid, J. Am. Ceram. Soc. 90 (2007) 950.
[19] K. Okawa, M. Sekine, M. Maeda, M. Tada, M. Abe, N. Matsushita, K. Nishio, H. Handa, J. Appl. Phys. 99 (2006) 08H102.
[20] E.S. Aazam, A.F. El-Husseiny, H.M. Al-Amri, Arabian J. Chem. (2010).
[21] L.A. Saghatforoush, R. Mehdizadeh, F. Chalabian, Trans. Met. Chem. 35 (2010) 903.
[22] R. Xu, T. Xie, Y. Zhao, Y. Li, Nanotechnology 18 (2007) 55602.
[23] H. Hu, K. Sugawara, Mater. Lett. 63 (2009) 940.
[24] P.K. Khanna, P.V. More, J.P. Jawalkar, B.G. Bharate, Mater. Lett. 63 (2009) 1384.
[25] Y.T. Jeon, J.Y. Moon, G.H. Lee, J. Park, Y. Chang, J. Phys. Chem. B 110 (2006) 1187.
[26] M. Han, Q. Liu, J.H. He, Y. Song, Z. Xu, J.M. Zhu, Adv. Mater. 19 (2007) 1096.
[27] P. Song, D. Wen, Z.X. Guo, T. Korakianitis, Phys. Chem. Chem. Phys. 10 (2008) 5057.
[28] Y. Du, H. Chen, R. Chen, N. Xu, Appl. Catal. A: Gen. 277 (2004) 259.
[29] M.H. Habibi, R. Mokhtari, M. Mikhak, M. Amirnasr, A. Amiri, Spectrochim. Acta A 79 (2011) 1524.
[30] M.H. Habibi, R. Kamrani, R. Mokhtari, Microchim. Acta 171 (2010) 91.
[31] J. Gao, F. Guan, Y. Zhao, W. Yang, Y. Ma, X. Lu, J. Hou, J. Kang, Mater. Chem. Phys. 71 (2001) 215.
[32] J.P. Costes, J.F. Lamère, C. Lepetit, P.G. Lacroix, F. Dahan, K. Nakatani, Inorg. Chem. 44 (2005) 1973.
[33] Y. Hou, H. Kondoh, T. Ohta, S. Gao, Appl. Surf. Sci. 241 (2005) 218.
[34] M.H. Habibi, R. Kamrani, R. Mokhtari, Microchim. Acta 171 (2010) 91–95.
[35] D.-H. Chen, C.-H. Hsieh, J. Mater. Chem. 12 (2002) 2412–2415.
[36] M. Wang, H. Li, Y. Wu, J. Zhang, Mater. Lett. 57 (2003) 2954.
[37] J.H. Hwang, V.P. Dravid, M.H. Teng, J.J. Host, B.R. Elliott, D.L. Johnson, T.O. Mason, J. Mater. Res. 12 (1997) 1076.
[38] X.M. Ni, Q.B. Zhao, H.G. Zheng, B.B. Li, J.M. Song, D.E. Zhang, X.J. Zhang, Eur. J. Inorg. Chem. 23 (2005) 4788.
[39] H.U. Blaser, Science 313 (2006) 312.
[40] A. Corma, P. Concepcion, P. Serna, Angew. Chem. Int. Ed. 46 (2007) 7266.
[41] X. Meng, H. Cheng, Y. Akiyama, Y. Hao, W. Qiao, Y. Yu, F. Zhao, S.I. Fujita, M. Arai, J. Catal. 264 (2009) 1.
[42] J.P. Ruparelia, A.K. Chatterjee, S.P. Duttagupta, S. Mukherji, Acta Biomater. 4 (2008) 707.
[43] M. Raffi, S. Mehrwan, T. Bhatti, J. Akhter, A. Hameed, W. Yawar, M. ul Hasan, Ann. Microbiol. 60 (2010) 75.